Journal of Cellular Biochemistry 98:701–705 (2006)

FAST TRACKS

Chaperone-Like Activity Revealed in the Matricellular Protein SPARC

Ryan O. Emerson,[1] E. Helene Sage,[3] Joy G. Ghosh,[1] and John I. Clark[1,2]*

[1]Department of Biological Structure, University of Washington, Seattle, WA 98195-7420
[2]Department of Ophthalmology, University of Washington, Seattle, WA 98195-7420
[3]Department of Vascular Biology, The Hope Heart Program,
the Benaroya Research Institute at Virginia Mason, 1201 Ninth Ave Seattle, WA 98101

Abstract SPARC (Secreted Protein, Acidic and Rich in Cysteine) is a matricellular glycoprotein that modulates cell proliferation, adhesion, migration, and extracellular matrix (ECM) production. In this report chaperone-like activity of SPARC was identified in a thermal aggregation assay in vitro. Ultraviolet circular dichroism (UVCD) spectroscopy determined that SPARC was stable at temperatures up to 50°C. Unfolding and aggregation of the chaperone target protein, alcohol dehydrogenase (ADH), were initiated at 50°C. SPARC inhibited the thermal aggregation of ADH in a concentration-dependent manner, with maximal inhibition at a 1:4 molar ratio of SPARC:ADH. Synergy between the chaperone-like activities of SPARC and αB-crystallin, a small heat shock protein and molecular chaperone in the lens, was observed in SPARC-αB-crystallin double −/− mice. J. Cell. Biochem. 98: 701–705, 2006.

Key words: SPARC; osteonectin; extracellular matrix; chaperone; αB-Crystallin

SPARC is a 32 kDa multifunctional protein consisting of 285 amino acids comprising three structural domains [Brekken and Sage, 2001]: An acidic N-terminal domain, a follistatin-like domain, and a Ca^{2+}-binding extracellular domain [Hohenester et al., 1996]. SPARC is expressed predominantly in remodeling tissues such as bone, healing wounds, and tumors [Sage et al., 1989; Reed and Sage, 1996], and modulates cellular interaction with the extracellular matrix (ECM) through interactions with proteins such as laminin [Sweetwyne et al., 2004] and collagen [Sasaki et al., 1997, 1998]. SPARC was observed in cell nuclei suggesting a direct effect on gene expression [Gooden et al., 1999]. Since a high-affinity SPARC receptor has not been identified, the various functions of SPARC appear to be mediated through the activity of receptors recognizing growth factors or other components of the ECM. Up-regulation of SPARC, and enhanced levels of SPARC mRNA, in response to heat-shock and other stresses have been described in transformed human keratinocytes [Kudo et al., 1994] and in chick chondrocytes [Neri et al., 1992] in vitro. Expression of SPARC was associated with cataract formation, a protein aggregation disease, in humans and in SPARC-null (−/−) mice [Gilmour et al., 1998; Norose et al., 1998; Bassuk et al., 1999; Kantorow et al., 2000], and a heat shock element was identified in the promoter regions of murine and bovine SPARC [Kudo et al., 1994]. We reasoned that a chaperone-like function of SPARC could account for its association with the stress response.

Under conditions of stress, proteins can become unfolded or misfolded and form large aggregates. Molecular chaperones protect against protein unfolding and aggregation. This report demonstrates the chaperone-like activity of SPARC in vitro.

MATERIALS AND METHODS

Circular Dichroism

The secondary structure of SPARC was determined by Ultraviolet Circular Dichroism

*Correspondence to: John I. Clark, PhD, 357420 Biological Structure, University of Washington, Seattle, WA 98195-7420. E-mail: clarkji@u.washington.edu

Received 1 January 2005; Accepted 15 August 2005
DOI 10.1002/jcb.20867

(UVCD) with a Jasco 720 circular dichroism spectrophotometer at three different experimental temperatures: 23, 37, and 50°C. Far-UV experiments were performed at a concentration of 0.1 mg/ml in 50 mM PBS, pH 7.0 with a 1 mm pathlength cuvette. Five accumulations were collected for each sample at each temperature. The far UVCD spectrum of the buffer (50 mM PBS, pH 7.0) was used for baseline correction. Data were collected between 250 and 200 nm. Below 200 nm, buffer absorption became too significant to allow accurate measurement.

Animals

Offspring of cross breeding of SPARC −/− with αB-crystallin −/− mice resulted in SPARC/αB-crystallin −/− mice that were examined by slit lamp. αB crystallin −/− mice were the generous gift of Dr. Eric Wawrousek, National Eye Institute [Brady et al., 2001]. 129SvEv x C57Bl/6J wild-type (wt, +/+) and SPARC-null (−/−) mice were generated as described previously [Norose et al., 1998]. Mice were housed in a modified pathogen-free facility by the University of Washington Department of Comparative Medicine under protocols and procedures approved by the University of Washington Animal Care and Use Committee that conform to the *Guide for the Care and Use of Laboratory Animals* published by the National Institutes of Health. Nonanesthetized mice were examined using a slit lamp biomicroscope (model FS-2; Nikon, Tokyo, Japan), as described previously [Alizadeh et al., 2004; Seeberger et al., 2004]. Mouse eyes were dilated with a 1:1 mixture of 1% tropicamide (Alcon, Fort Worth, TX) and 10% phenylephrine hydrochloride (Akorn, Abita Springs, LA). The angle of the slit lamp was approximately 40°, and the slit width was approximately 0.2 mm. Examinations were recorded by digital video (Canon Optura Pi, Tokyo, Japan). Still images were captured (Premiere; Adobe, San Diego, CA) and processed (Photoshop; Adobe).

Chaperone Assays

Aggregation of ADH (Alcohol Dehydrogenase from equine liver, lot 093K7400; Sigma, St. Louis, MO) was measured spectrophotometrically as apparent OD_{360} (Optical Density, 360 nm) at 50°C for up to 120 min by the use of a Pharmacia Ultrospec 3000 multisample UV/Vis spectrometer fitted with a VWR model 1160 circulating bath. Temperature was controlled to +/− 0.1°C. OD was recorded every 2 min and was plotted as ΔOD, where $\Delta OD_t = OD_t - OD_0$. The values of ΔOD for each sample were normalized as follows: $(\Delta OD_t - \Delta OD_b)/\Delta OD_{max}$, where ΔOD_b = the ΔOD_t for the buffer blank at the same time point and ΔOD_{max} = the maximum ΔOD_t across all time points and samples in an experiment. The normalized ΔOD values were used for the figures. All solutions were prepared using 150 mM PBS (50 mM sodium phosphate buffer, pH 7.0, in 0.1 M NaCl). ADH was present at a concentration of 0.5 mg/ml, and the total volume in all cases was 0.1 ml. Recombinant human αB-crystallin was produced in *E. coli* as described previously [Muchowski et al., 1997]. Recombinant human SPARC was produced as described [Bradshaw et al., 2000]. Briefly, SPARC cDNA was cloned into a baculovirus expression vector, after which protein was produced by virally-transfected *S. frugiperda* cells. Protein was purified on an anion-exchange column, followed by gel filtration chromatography. Purity was estimated at >97% by SDS-PAGE. All protein concentrations were measured using the BCA Protein assay kit (Pierce, Rockford, IL).

RESULTS

The stability of SPARC in response to thermal stress was determined using UVCD to evaluate the secondary structure of SPARC at high temperature (Fig. 1). The minimum absorbance observed in the UVCD spectrum at 220 nm indicated α-helical structure. Heating SPARC to 50°C produced an increased molar ellipticity peak at 215 nm but otherwise left the spectrum unchanged. Protein aggregation measured by OD had a characteristic S-shaped form [Kodaka, 2004; Fig. 2]. The initial slope near zero corresponded with activation that initiated nucleation of aggregates as a result of conformational changes induced by high temperature. Continued growth in the number and size of the aggregates corresponded with an increased slope. An inflection point was observed when aggregation approached equilibrium.

In the presence of a 1:8 molar ratio of SPARC:ADH, the maximum ΔOD decreased approximately 80%, and in the presence of a 1:20 molar ratio of SPARC:ADH, the maximum ΔOD decreased approximately 45%. The molar

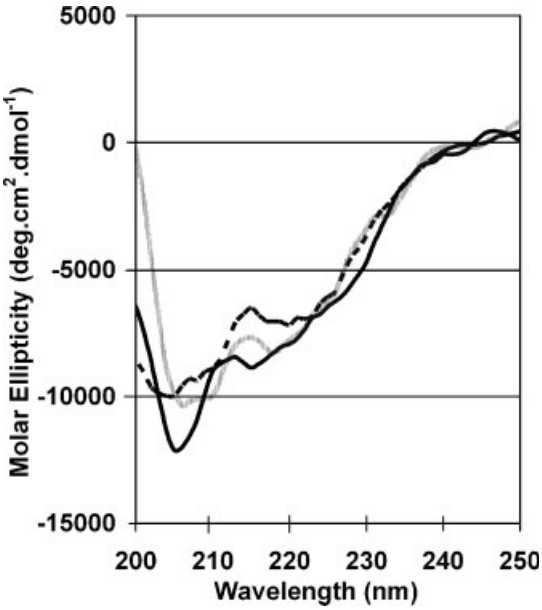

Fig. 1. Thermal stability of SPARC. Ultraviolet circular dichroism (UVCD) spectra of 0.1 mg/ml SPARC at 25°C (solid gray line), 37°C (solid black line), and 50°C (dashed black line). Mean residue molar ellipticity, calculated as $\deg \cdot cm^2 \cdot dmol^{-1}$, is plotted against wavelength. The minimum observed near 220 nm is representative of α-helical structure, and remains constant up to 50°C. No significant differences in the patterns of spectra at 23°C, 37°C and 50°C were observed. The secondary structure of SPARC appears to be stable up to 50°C.

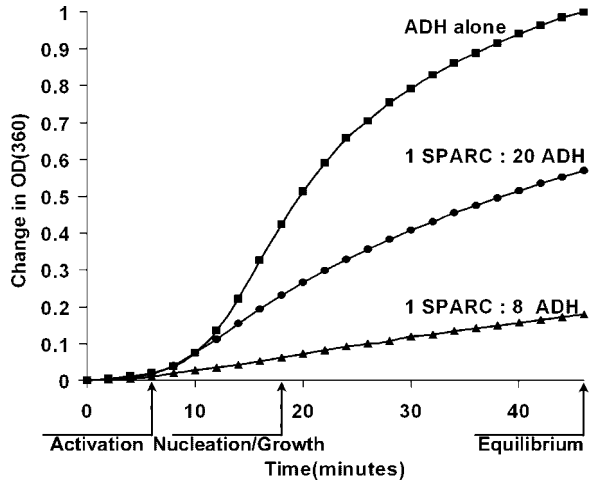

Fig. 2. SPARC inhibited the thermal aggregation of ADH. Optical density (OD) was plotted against time for ADH alone (■), and ADH with molar ratios of SPARC:ADH of 1:20 (○) and 1:8 (▲). In the presence of a 1:20 molar ratio of SPARC:ADH, the maximum observed OD decreased approximately 45%. In the presence of 1:8 of SPARC:ADH, the maximum observed OD decreased approximately 80%. All curves were S-shaped, with an activation phase with little change, followed by a growth period of increasing slope and then an inflection point as aggregation approached equilibrium. The length of the activation and growth phases was similar in the presence and absence of SPARC. Increasing the concentration of SPARC was correlated with decreasing aggregation of ADH at 50°C. OD was normalized as described in Methods.

ratio of SPARC:ADH required for maximum inhibition of ADH aggregation was less than the molar ratio of αB-crystallin:ADH required for maximum inhibition of ADH aggregation (Fig. 3). In the presence of a 1:4 molar ratio of SPARC:ADH, inhibition of ADH thermal aggregation was nearly complete, and the same inhibition required a molar ratio of 2:1, αB-crystallin:ADH (data not shown). The effect of αB-crystallin was on the initial part of the aggregation curve defined as the time from intercept on the Y-axis to beginning of the increase in slope. In contrast, SPARC had no measurable effect on the initial part of the aggregation curve.

The combined effect of the deletion of SPARC and αB-crystallin on lens transparency was dramatic. In SPARC/αB-crystallin double −/− mice, opacification was accelerated and a mature opacity developed by 1 month of age (Fig. 4).

DISCUSSION

The results demonstrated that SPARC has chaperone-like activity in vitro. The presence of SPARC inhibited thermal aggregation of ADH. The chaperone-like activity of SPARC was stronger than that of the small heat shock protein and molecular chaperone αB-crystallin, on the basis of the molar ratios necessary to suppress ADH aggregation. In the absence of

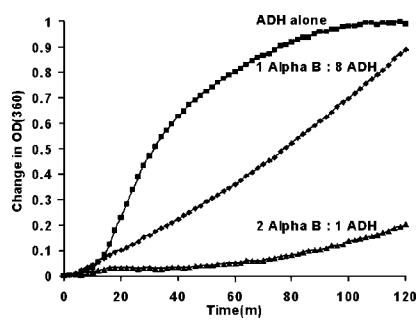

Fig. 3. The effect of αB-crystallin on the thermal aggregation of ADH. Optical density was plotted against time for ADH alone (■), and ADH with molar ratios of αB-crystallin:ADH of 1:8 (●) and 2:1 (▲). Complete inhibition of aggregation was observed in the presence of 2:1 αB-crystallin:ADH. Partial inhibition was observed with a 1:8 molar ratio of αB-crystallin:ADH. αB-crystallin significantly increased the amount of time to the observed inflection point without decreasing the maximum observed OD.

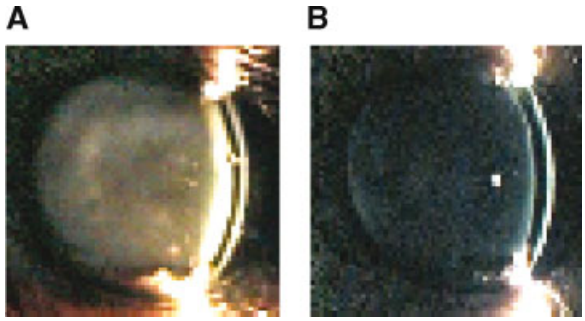

Fig. 4. Cataract formation in SPARC-αB-crystallin double −/− mice. Slit lamp views of the eyes of 1-month-old SPARC/αB-crystallin −/− mice (**A**) and a 1 month old SPARC −/− mouse (**B**). The lenses in the SPARC/αB-crystallin double −/− mice contained a mature opacity at 1 month of age when lenses in SPARC −/− mice (B) were as clear as those of αB-crystallin −/− or wt mice. The dense opacity was observed throughout the entire lens and was not present at birth. In contrast, SPARC −/− mice develop dense opacity by 6 months of age. αB-crystallin −/− mice develop mild opacities with age that are similar to aging cataract in wt mice. [Color figure can be viewed in the online issue, which is available at www.interscience.wiley.com.]

SPARC, the opacification in αB-crystallin −/− mice was accelerated. UVCD demonstrated that SPARC retained secondary structure and conformation at high temperature, with only minor differences noted between the UVCD spectra for SPARC at 23°C and SPARC at 50°C. This finding supported the stability of SPARC as a chaperone and the hypothesis that SPARC could be a stress protein in vivo.

The effect of SPARC was on the OD reached at equilibrium. In contrast, the effect of αB-crystallin was on the length of the activation and growth phases of the ADH aggregation curve. The difference in the effects on the aggregation curves suggested that the mechanism of SPARC as a molecular chaperone may be different from that of αB-crystallin and will be investigated in future experiments.

The appearance of mature opacities at only 1 month of age in SPARC/αB-crystallin double −/− mice reinforced the previous finding (11–14) that SPARC was necessary for normal lens transparency during aging, and demonstrated the possibility of a synergistic effect between molecular chaperones having separate mechanisms of action. Each chaperone may be important but not required for lens transparency. The combined impact of the absence of both chaperones on misfolded proteins may accelerate protein aggregation and loss of normal transparency at an early age.

ACKNOWLEDGMENTS

Support from NEI grant EY13180 and NIH grant GM40711, and technical assistance from Ms. G. Workman and Mr. E. Arnett are gratefully acknowledged.

REFERENCES

Alizadeh A, Clark JI, Seeberger TM, Hess J, Blankenship T, Fitsgerald PG. 2004. Characterization of a mutation in the lens specific CP49 in the 129 strain of mouse. Invest Opthalmol Vis Sci 45:884–892.

Bassuk JA, Birkebak T, Rothmier JD, Clark JM, Bradshaw A, Muchowski PJ, Howe CC, Clark JI, Sage H. 1999. Disruption of the Sparc locus in mice alters the differentiation of lenticular epithelial cells and leads to cataract formation. Exp Eye Res 68:321–331.

Bradshaw AD, Bassuk JA, Fancki A, Sage EH. 2000. Expression and purification of recombinant human SPARC produced by baculovirus. Mol Cell Biol Res 3: 345–351.

Brady JP, Garland DL, Green DE, Tamm ER, Giblin FJ, Wawrouesk EF. 2001. aB-Crystallin in lens development and muscle integrity: A gene knockout approach. Invest Opthalmol Vis Sci 42:2924–2934.

Brekken RA, Sage EH. 2001. SPARC, a matricellular protein: At the crossroads of cell-matrix communication. Matrix Biol 19:816–827.

Gilmour DT, Lyon GJ, Carlton MB, et al. 1998. Mice deficient for the secreted glycoprotein SPARC/osteonectin/BM40 develop normally but show severe age-onset cataract formation and disruption of the lens. EMBO J 17:1860–1870.

Gooden MD, Vernon RB, Bassuk JA, Sage EH. 1999. Cell cycle-dependent nuclear location of the matricellular protein SPARC: Association with the nuclear matrix. J Cell Biochem 74:152–167.

Hohenester E, Maurer P, Hohenadl C, Timpl R, Jansonius JN, Engel J. 1996. Structure of a novel extracellular Ca(2+)-binding module in BM-40. Nat Struct Biol 3:67–73.

Kantorow M, Huang Q, Yang XJ, Sage EH, Magabo KS, Miller KM, Horwitz J. 2000. Increased expression of osteonectin/SPARC mRNA and protein in age-related human cataracts and spatial expression in the normal human lens. Mol Vis 6:24–29.

Kodaka M. 2004. Requirements for generating sigmoidal time-course aggregation in nucleation-dependent polymerization model. Biophys Chem 107:243–253.

Kudo H, Hirayoshi K, Kitagawa Y, Imamura S, Nagata K. 1994. Two collagen-binding proteins, osteonectin and HSP47, are coordinately induced in transformed keratinocytes by heat and other stresses. Exp Cell Res 212: 219–224.

Muchowski PJ, Bassuk JA, Lubsen NH, Clark JI. 1997. Human alphaB-crystallin: Small heat shock protein and molecular chaperone. J Biol Chem 272:2578–2582.

Neri M, Descalzi-Cancedda F, Cancedda R. 1992. Heat-shock response in cultured chick embryo chondrocytes. Osteonectin is a secreted heat-shock protein. Eur J Biochem 205:569–574.

Norose K, Clark JI, Syed NA, Basu A, Heber-Katz E, Sage EH, Howe CC. 1998. SPARC deficiency leads to

early-onset cataractogenesis. Invest Opthalmol Vis Sci 39: 2674–2680.

Reed MJ, Sage EH. 1996. SPARC and the extracellular matrix: Implications for cancer and wound repair. Curr Top Microbiol Immunol 213:81–94.

Sage EH, Vernon RB, Decker J, Funk S, Iruela-Arispe ML. 1989. Distribution of the calcium-binding protein SPARC in tissues of embryonic and adult mice. J Histochem Cytochem 37:819–829.

Sasaki T, Gohring W, Mann K, et al. 1997. Limited cleavage of extracellular matrix protein BM-40 by matrix metalloproteinases increases its affinity for collagens. J Biol Chem 272:9237–9243.

Sasaki T, Hohenester E, Gohring W, Timpl R. 1998. Crystal structure and mapping by site-directed mutagenesis of the collagen-binging epitope of an activated form of BM-40/SPARC/osteonectin. EMBO J 17:1625–1634.

Seeberger TM, Matsumoto Y, Alizadeh A, Fitzgerald PG, Clark JI. 2004, Digital imagecapture and quantification of subtle lens opacities in rodents. J Biomed Opt 9:116–120.

Sweetwyne MT, Brekken RA, Workman G, Bradshaw AD, Carbon J, Siadak AW, Murri C, Sage EH. 2004. Functional analysis of the matricellular protein SPARC with novel monoclonal antibodies. J Histochem Cytochem 52:723–733.